

Supporting Information

Selectively decorated Ti-FeOOH co-catalyst for a highly efficient hematite-based water splitting system

Ki-Yong Yoon, Hyo-Jin Ahn, Myung-Jun Kwak, Sun-I Kim, Juhyung Park, and

Ji-Hyun Jang*

School of Energy and Chemical Engineering, Low Dimensional Carbon Materials Center,

Ulsan National Institute of Science and Technology, Ulsan 44919, Republic of Korea

Experimental

Reagents.

Ferric chloride hexahydrate ($\text{FeCl}_3 \cdot 6\text{H}_2\text{O}$, KANTO CHEMICAL CO., INC., 99.0%), Titanium trichloride (TiCl_3 , SIGMA-ALDRICH, assay $\geq 12\%$), 3-(aminopropyl) trimethoxysilane (APTMS, SIGMA-ALDRICH, assay: 97%).

Preparation of the Ti-H photoanode.

Ti-doped $\alpha\text{-Fe}_2\text{O}_3$ (Ti-H) photoanode was grown on fluorine-doped tin oxide (FTO) glass by previously reported aqueous chemical growth method followed by a rapid inserted annealing process. The experiment was performed in an aqueous solution containing 100 mL of 150 mM Ferric chloride hexahydrate ($\text{FeCl}_3 \cdot 6\text{H}_2\text{O}$) and 7 μl of titanium trichloride (TiCl_3). The solution was placed in cap-sealed glass vial containing two back-to-back slips of FTO glass leaning against the inner wall. The glass vial was placed in a forced convection oven with a programmable temperature controller. The increased pressure due to the creation of HCl and water vapor gas did not cause any explosion under our experimental conditions (we obtained similar results to the case of using a pressure-sustainable autoclave). After heating to 100 °C from 30 °C for 2 hours, the temperature was maintained for 3 hours, during which Ti-doped FeOOH rods were synthesized on the FTO substrate. The sample is thoroughly washed by water and dried by N_2 gas. The Ti-FeOOH on the FTO substrate was rapidly inserted into a furnace tube at 850 °C for 20 min and taken out to the ambient conditions.

Preparation of the Ti-PH photoanode.

The 3-(aminopropyl) trimethoxysilane (APTMS) solution was made by mixing DI

water:APTMS =100:1(v:v). Ti-FeOOH grown on the FTO substrate was immersed in the APTMS solution for 30 min. After washing the sample by DI water and drying by N₂ gas, Ti-FeOOH was annealed by the same method (rapidly inserted into a furnace tube at 850 °C for 20 min and taken out to the ambient conditions) as used for the preparation of Ti-H to create hematite with pores inside and a SiO_x layer outside.

Preparation of the FeOOH/Ti-PH or Ti-FeOOH/Ti-PH photoanode.

In order to decorate undoped FeOOH co-catalyst on Ti-PH, Ti-PH was immersed in a 1.5 mM of ferric chloride hexahydrate solution for 30 min at 70 °C. For Ti-FeOOH/Ti-PH, Ti-PH was immersed in a mixture of 100 mL of 1.5 mM ferric chloride hexahydrate and 7 ul of titanium trichloride solutions, and the sample was heated to 70 °C by maintaining the temperature for 30 min. After growing the co-catalyst, the photoanode was washed with DI water and dried by N₂ gas.

PEC measurement.

A three-electrode configuration with front-side simulated AM 1.5 illumination was used for PEC measurement, composed of an Ag/AgCl (KCl sat.) electrode and a Pt mesh as reference and counter electrodes, respectively. An exposed area of the photoanode was 0.44 cm² made by the O-ring. A 1.0 M NaOH solution was used as a pH 13.6 electrolyte. Potential versus RHE were calculated using the Nernst equation $E_{\text{RHE}} = E_{\text{Ag/AgCl}} + 0.0591(\text{pH}) + 0.1976 \text{ V}$. The scan rate for J-V curve was 20 mVs⁻¹. Photocurrent stability tests were carried out by measuring photocurrent produced under AM 1.5 at a fixed electrode potential of 1.23 V vs RHE. EIS was carried out at a frequency range from 100 kHz to 0.1 Hz using a potentiostat. EIS experimental data were analyzed and fitted using the Zview software and IPCE

measurement was carried out under monochromatic light by a Xe lamp providing illumination through a monochromator. The illumination intensity of the monochromatic light was measured by a luminometer.

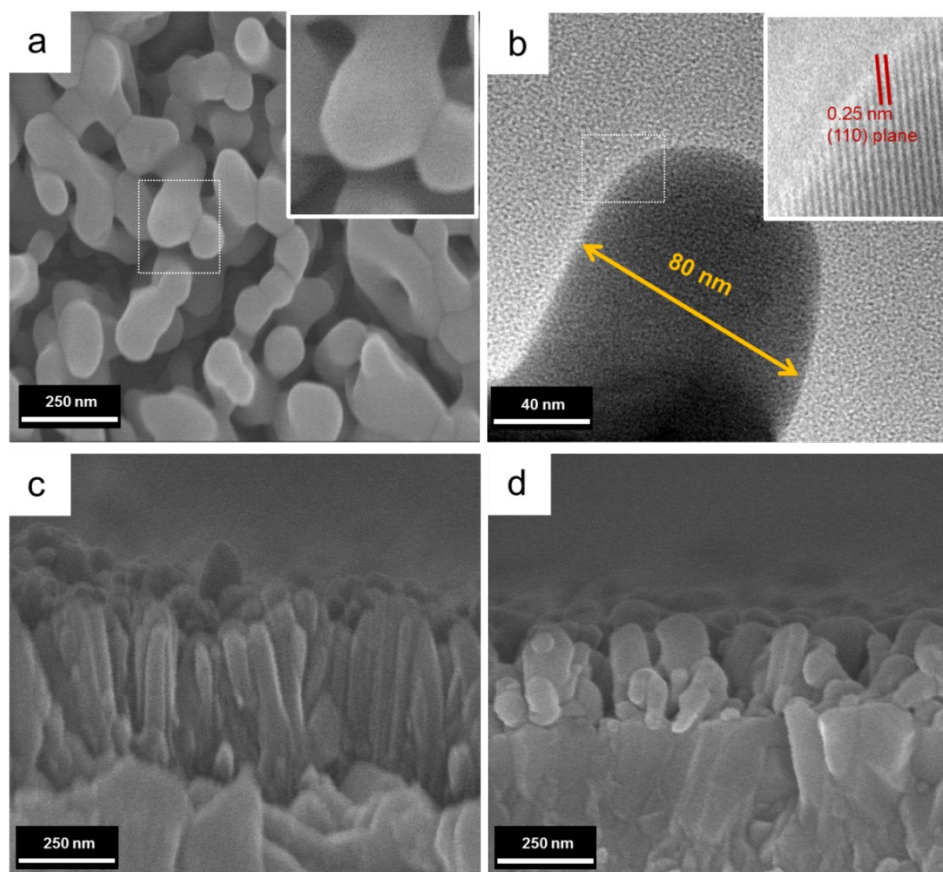


Figure S1. a) Scanning electron microscope (SEM) image and b) transmission electron microscopy (TEM) image of Ti-H. The inset is the high resolution image of the dotted rectangle region in each image. Cross-view SEM image of c) Ti-FeOOH and d) Ti-H.

The reference sample, Ti-H, is a rod structure with a diameter of 80-100 nm and overall height of 250-300 nm. The (110) planes of Ti-H corresponding to the lattice spacing of 0.25

nm, which allows a 4 order of magnitude higher conductivity than that of the perpendicular direction, identify the fabrication of worm-like α -Fe₂O₃.

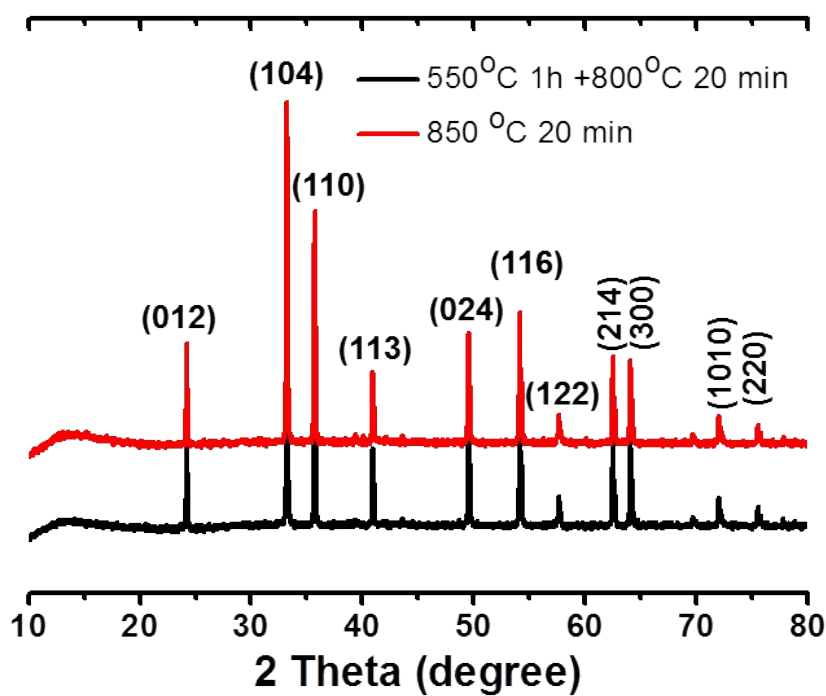


Figure S2. Comparison of XRD patterns for conventional annealing (550 °C 1h+800 °C 20 min) and rapidly inserted annealing (850 °C 20 min).

Fe₂O₃ fabricated by two different annealing methods shows similar typical hematite peaks.

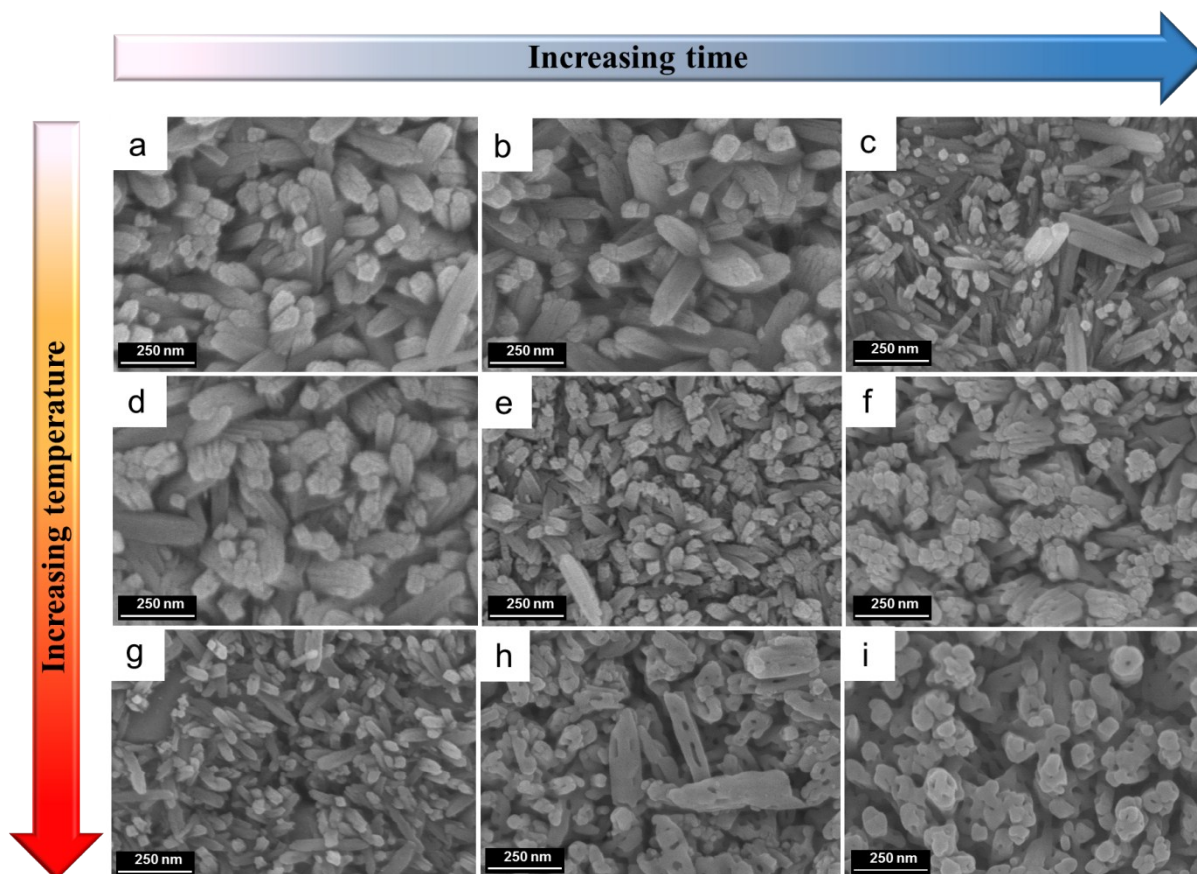


Figure S3. SEM images of different annealing conditions of different times and various temperatures. The duration of annealing increases from left to right whereas the temperature of annealing increases from top to bottom, as indicated by the arrows. a-c) Ti-PH prepared with annealing for 5, 10, and 20 min at 650 °C temperature. d-f) Ti-PH prepared with annealing for 5, 10, and 20 min at 750 °C temperature. g-i) Ti-PH prepared with annealing for 5, 10, and 20 min at 850 °C. Pores are observed only in f, h, and i, where the samples underwent severe annealing conditions to create enough internal pressure for pore generation.

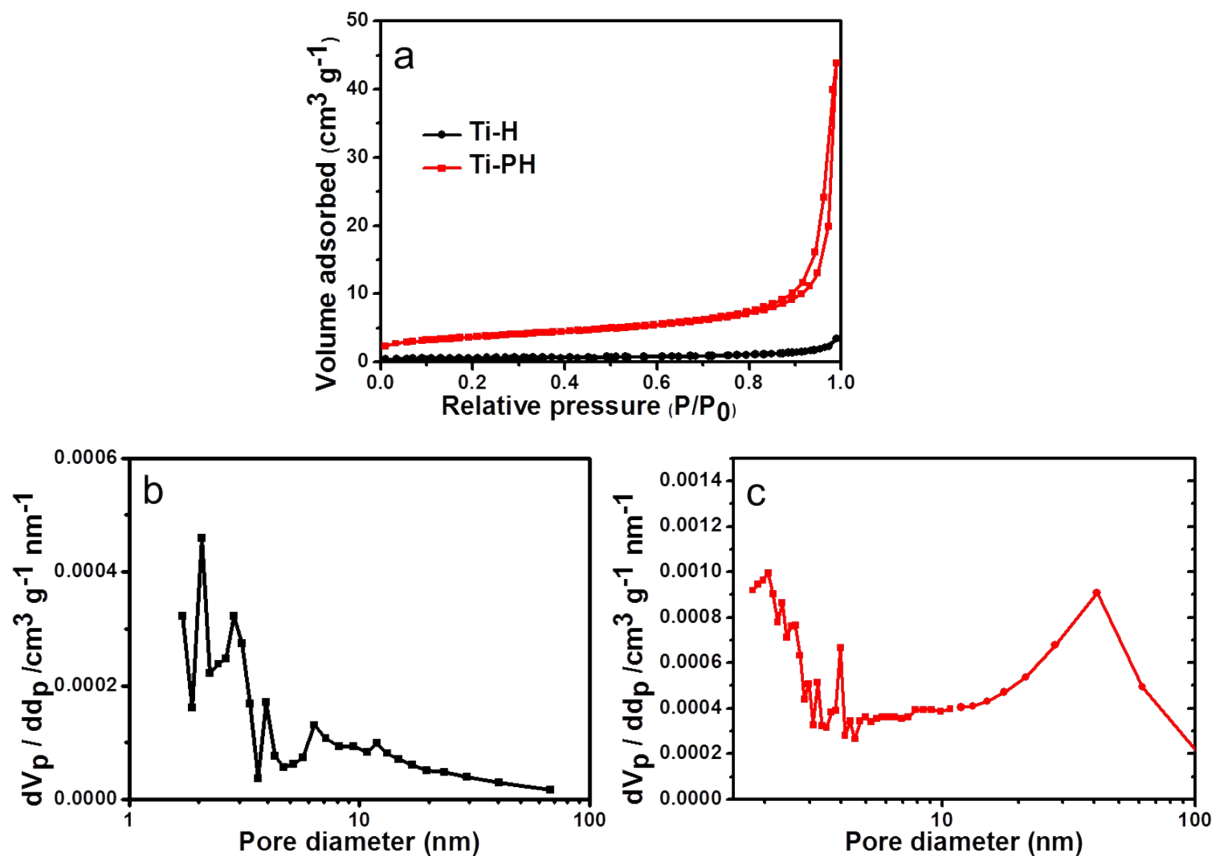


Figure S4. N₂ adsorption-desorption isotherms of two kinds of hematite. The BET surface area of Ti-H is 2 m²/g and Ti-PH is 12 m²/g. The pore distribution of b) Ti-H and c) Ti-PH.

From the BET isotherm and Barrett-Joyner-Halenda (BJH) pore distribution plots, we confirmed that the presence of mesopores in Ti-PH. Mesopores are likely from the gas entrapping. The surface area of Ti-PH is increased six-fold compared to that of Ti-H.

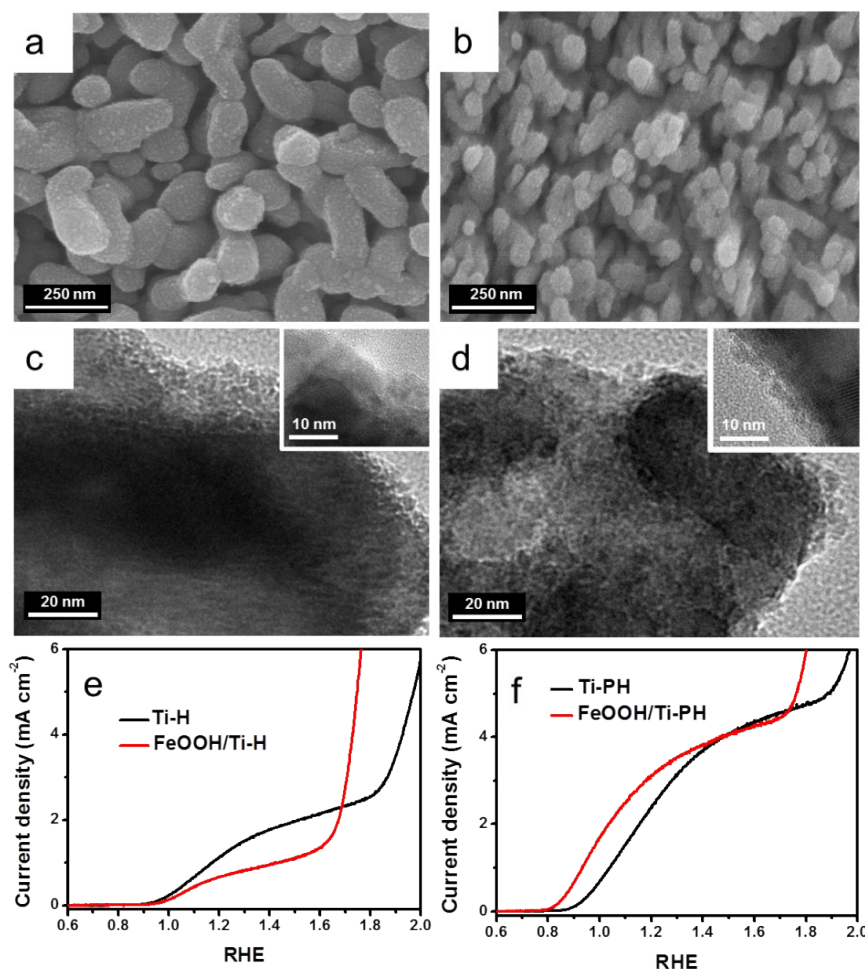


Figure S5. SEM images of a) FeOOH/Ti-H by using 1.5 mM FeCl₃ and b) FeOOH/Ti-PH by using 1.5 mM FeCl₃. TEM images of c) FeOOH/Ti-H and d) FeOOH/Ti-PH. J-V curves under simulated sunlight illumination in the 1 M NaOH (pH=13.6) electrolyte of c) FeOOH/Ti-H and d) FeOOH/Ti-PH.

The diameters of FeOOH/Ti-H rods are greater than those of Ti-H rods due to the high density decoration of the FeOOH catalyst on Ti-H (without both pores and the SiO_x layer), as shown in Figure S5 (a and c). In contrast, the thickness of FeOOH/Ti-PH (b and d) was almost maintained after FeOOH deposition, since the outer SiO_x surface of Ti-PH interrupted the easy decoration of FeOOH catalysts on the surface of Ti-PH (with both pores and the SiO_x layer). As a result, the photocurrent density of FeOOH/Ti-H was lowered after FeOOH deposition due to the competition of light intensity (e), whereas that of FeOOH/Ti-PH was improved after FeOOH decoration (f) due to the properly working co-catalytic effect of FeOOH.

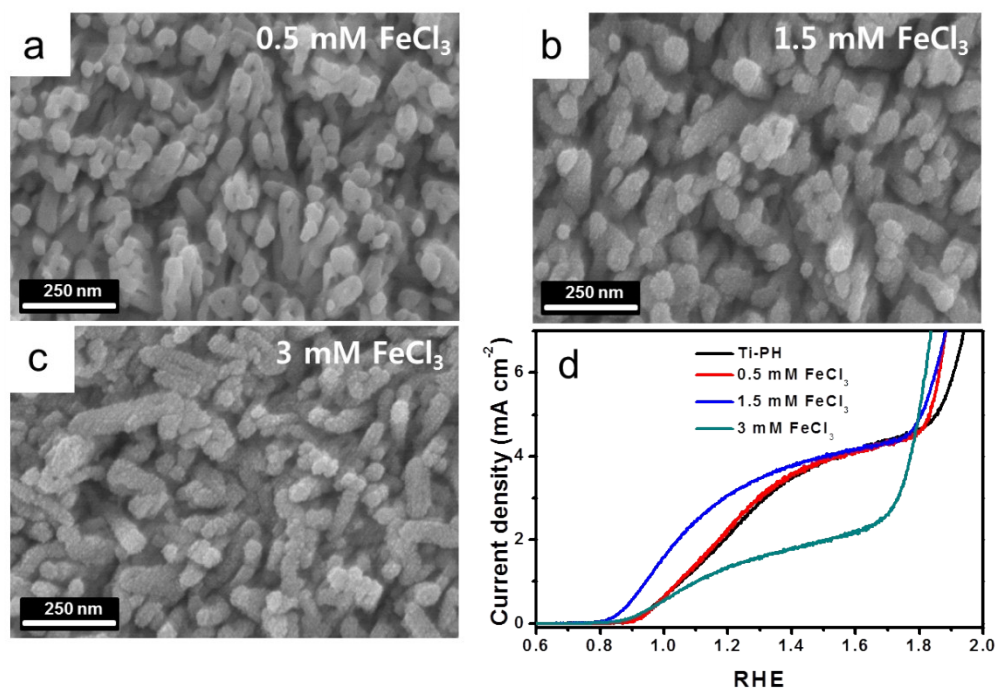


Figure S6. SEM images and PEC performance of FeOOH/Ti-PH prepared by using different FeCl₃ concentrations: a) 0.5 mM FeCl₃, b) 1.5 mM FeCl₃ and c) 3 mM FeCl₃. d) J-V curves under simulated sunlight illumination in a 1 M NaOH (pH=13.6) electrolyte, which confirms that FeOOH/Ti-PH obtained by simply lowering the concentration of co-catalysts (0.5 mM FeCl₃) does not present the optimized photocurrent density values.

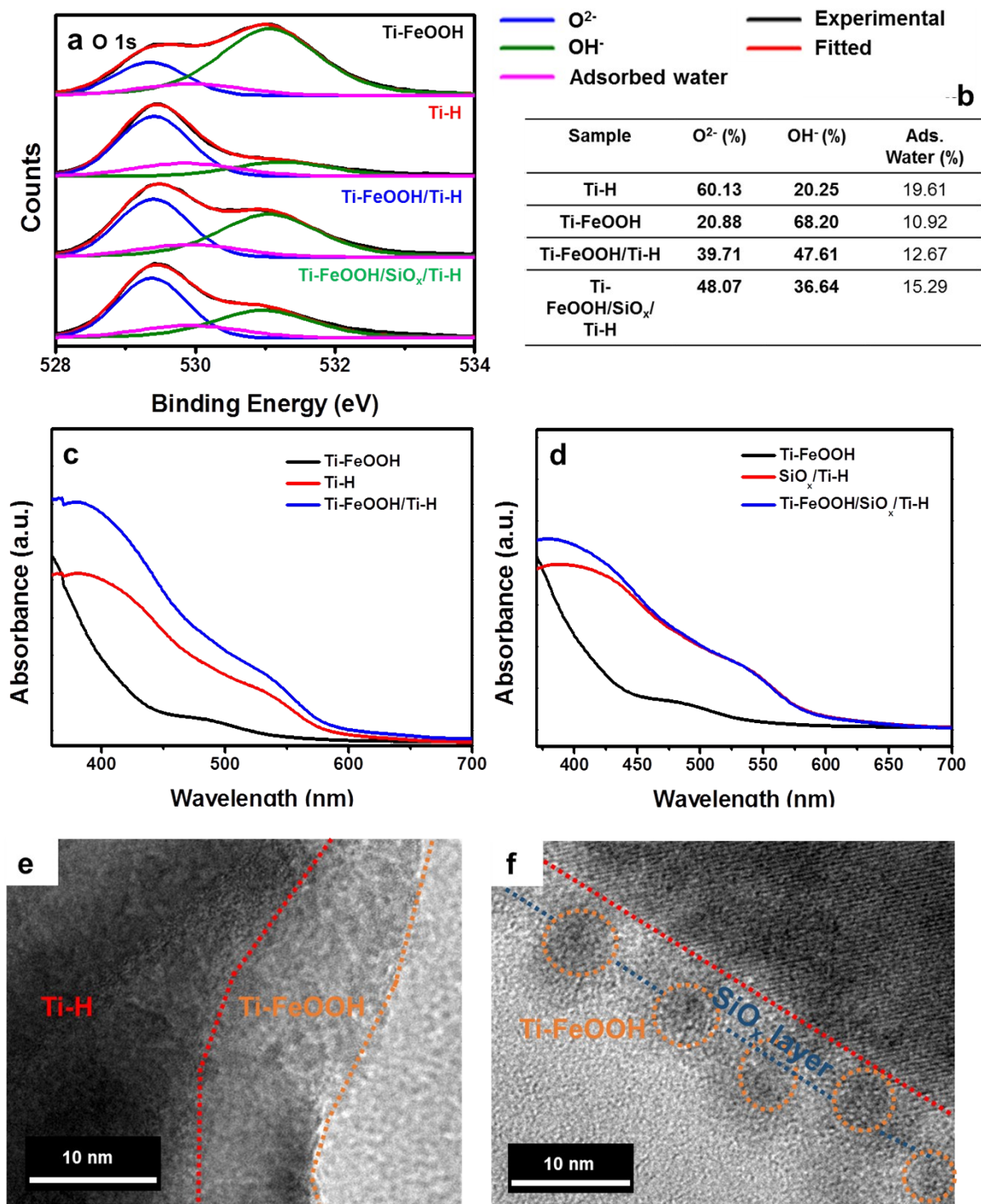


Figure S7. O 1s XPS spectra a) of Ti-FeOOH, Ti-H, Ti-FeOOH/Ti-H, and Ti-FeOOH/SiO_x/Ti-H. b) Relative portion of each component by deconvolution of O 1s peaks. UV-VIS absorption spectra of c) Ti-FeOOH/Ti-H and d) Ti-FeOOH/SiO_x/Ti-H. TEM images of e) Ti-FeOOH/Ti-H and f) Ti-FeOOH/SiO_x/Ti-H.

In order to clearly prove the preferential deposition of Ti-FeOOH on the inner surface of Ti-PH, we made non porous hematite (Ti-H) w/wo the SiO_x layer using 150 mM FeCl₃ solution.^[1] SiO_x/Ti-H was made by APTMS treatment on Ti-H. After the same hydrothermal deposition of Ti-FeOOH on SiO_x/Ti-H and Ti-H, we compared the XPS and UV-Visible absorption data of Ti-FeOOH/SiO_x/Ti-H and Ti-FeOOH/Ti-H. The O 1s peaks in the XPS spectra (Figure S7a) show that the Ti-FeOOH co-catalyst has a rich OH⁻ peak (68%) and poor O²⁻ peak (21%) in comparison with Ti-Fe₂O₃ (Ti-H) with the 20% of OH⁻ peak and 60% of O²⁻ peak. Therefore, the higher intensity of the OH⁻ peak and the lower intensity of the O²⁻ peak in Ti-FeOOH/Ti-H than in Ti-FeOOH/SiO_x/Ti-H suggest that there is a larger amount of Ti-FeOOH on the surface of Ti-H than on the surface of SiO_x/Ti-H (Figure S7a-b), which confirms the preferential deposition of Ti-FeOOH on Fe₂O₃. As shown in Figures S7c-d, UV-VIS absorption spectra also confirm the preferential deposition of Ti-FeOOH on Ti-H rather than SiO_x/Ti-H. Even though the same deposition procedure was used, FeOOH/Ti-H showed greatly enhanced absorption by Ti-FeOOH in the range of 320-580 nm, where Ti-FeOOH had a strong absorption intensity, whereas Ti-FeOOH/SiO_x/Ti-H exhibited a slightly enhanced absorption. In addition, the TEM image in Figure S7e shows that Ti-FeOOH co-catalysts were readily deposited on the surface of Ti-H, forming a layer-like morphology. On the other hand, 2-4 nm Ti-FeOOH particles were sparsely deposited on the surface of SiO_x/Ti-H as shown in Figure S7f.

[1] J.-W. Jang, C. Du, Y. Ye, Y. Lin, X. Yao, J. Thorne, E. Liu, G. McMahon, J. Zhu, A. Javey, J. Guo, D. Wang, Nat Commun 6 (2015).

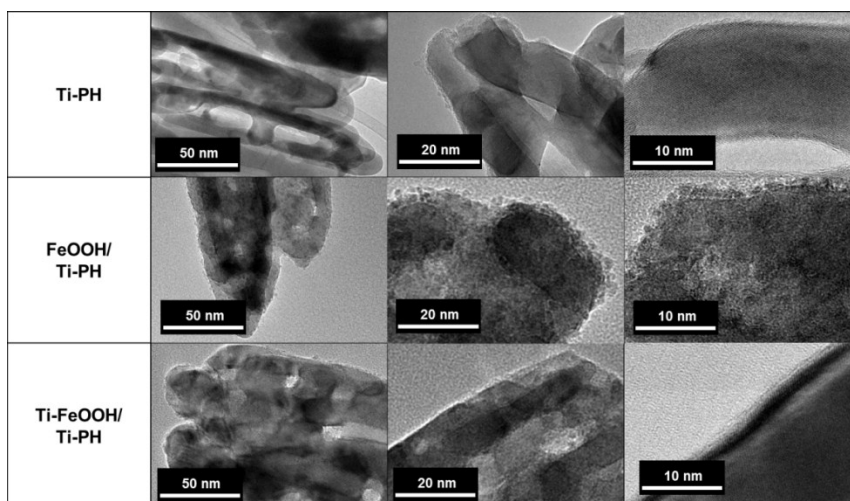


Figure S8. TEM images of Ti-PH, FeOOH/Ti-PH and Ti-FeOOH/Ti-PH.

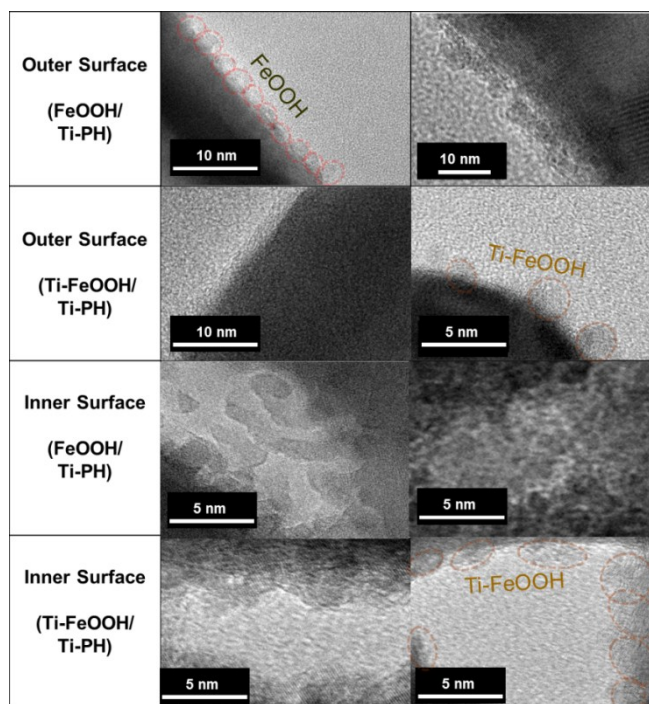


Figure S9. TEM images of FeOOH/Ti-PH and Ti-FeOOH/Ti-PH that confirm the different deposition densities of co-catalysts on the outer and inner surface of Ti-PH. Ti-FeOOH was deposited by our synthetic method (with 1.5 mM FeCl_3).

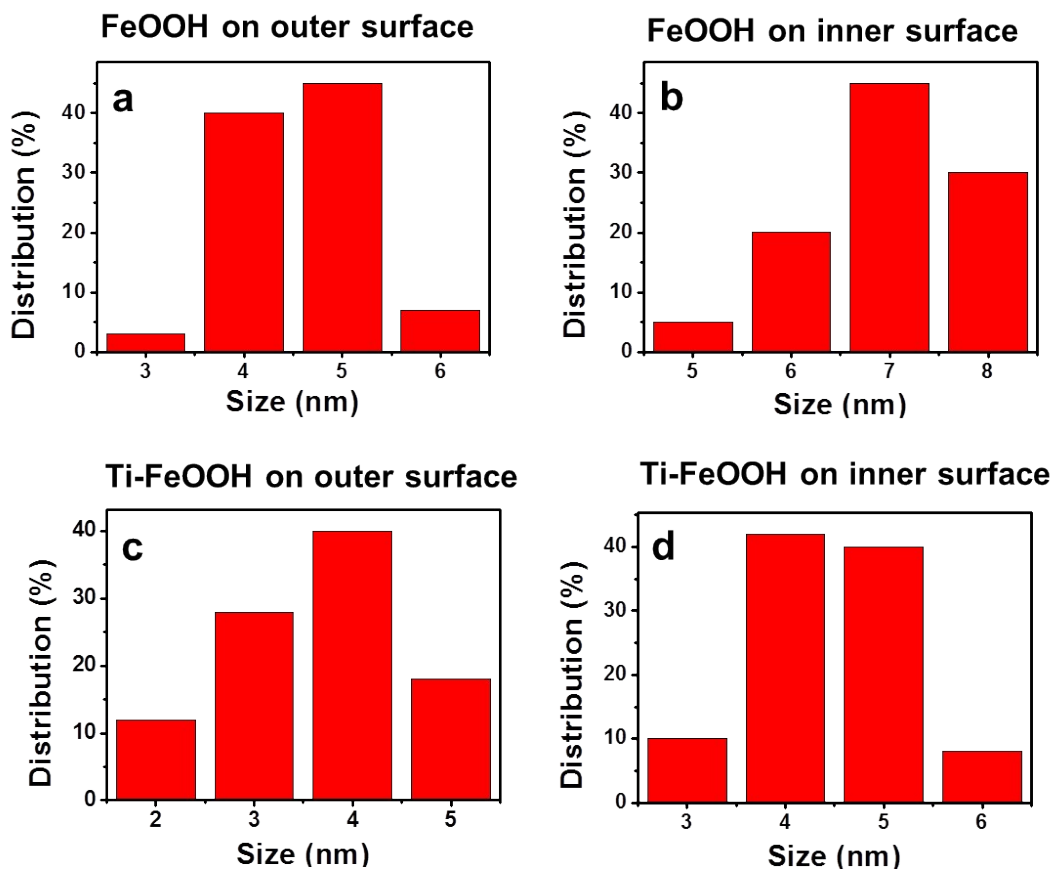


Figure S10. Statistic histogram of FeOOH particles size distribution on a) outer and b) inner surface of Ti-PH and Ti-FeOOH particles size distribution on c) outer and d) inner surface of Ti-PH.

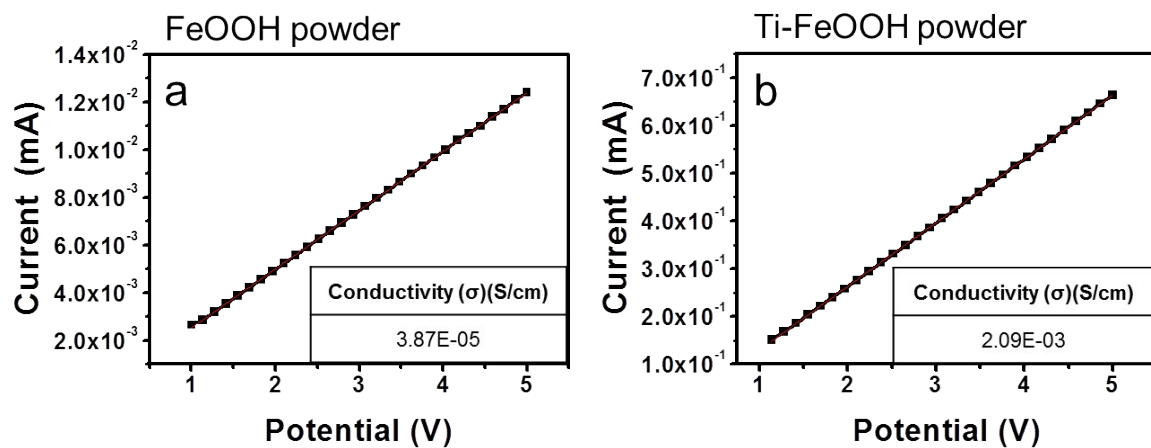


Figure S11. Powder conductivity measurements. a) FeOOH and b) Ti-FeOOH.

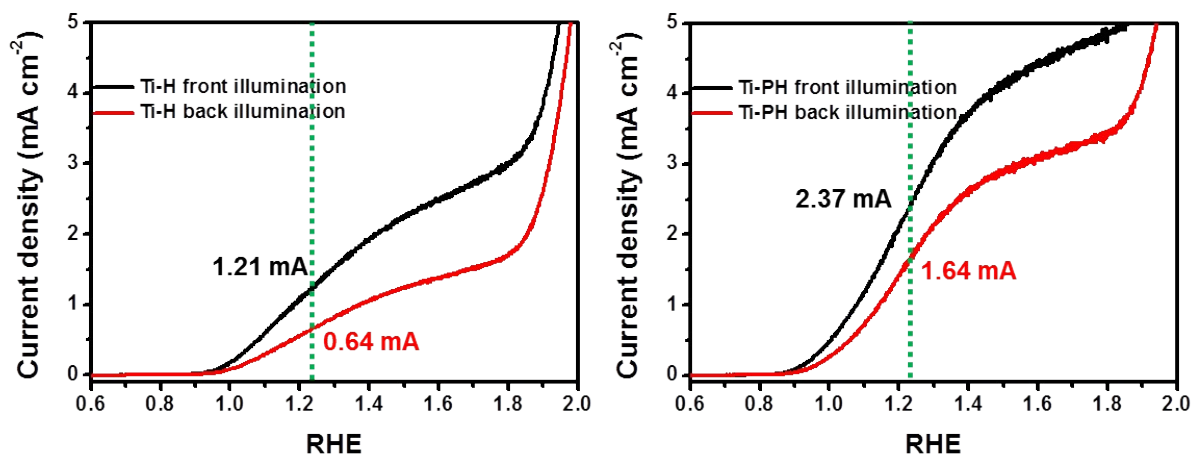


Figure S12. J-V curves a) Ti-H and b) Ti-PH under simulated sunlight front and back illumination (1 SUN) in 1 M NaOH electrolyte.

In the case of Ti-H, back-side illumination results in a 47.1 % reduction of photocurrent compared with front-side illumination (a). On the contrary, back-side illumination of Ti-PH reduced the photocurrent density by 30.8% compared to that of front-side illumination (b). The lower disparity in the performance between front/back illumination of Ti-PH compared to Ti-H confirms the reduced path distance of holes for water oxidation reactions in the porous structure.

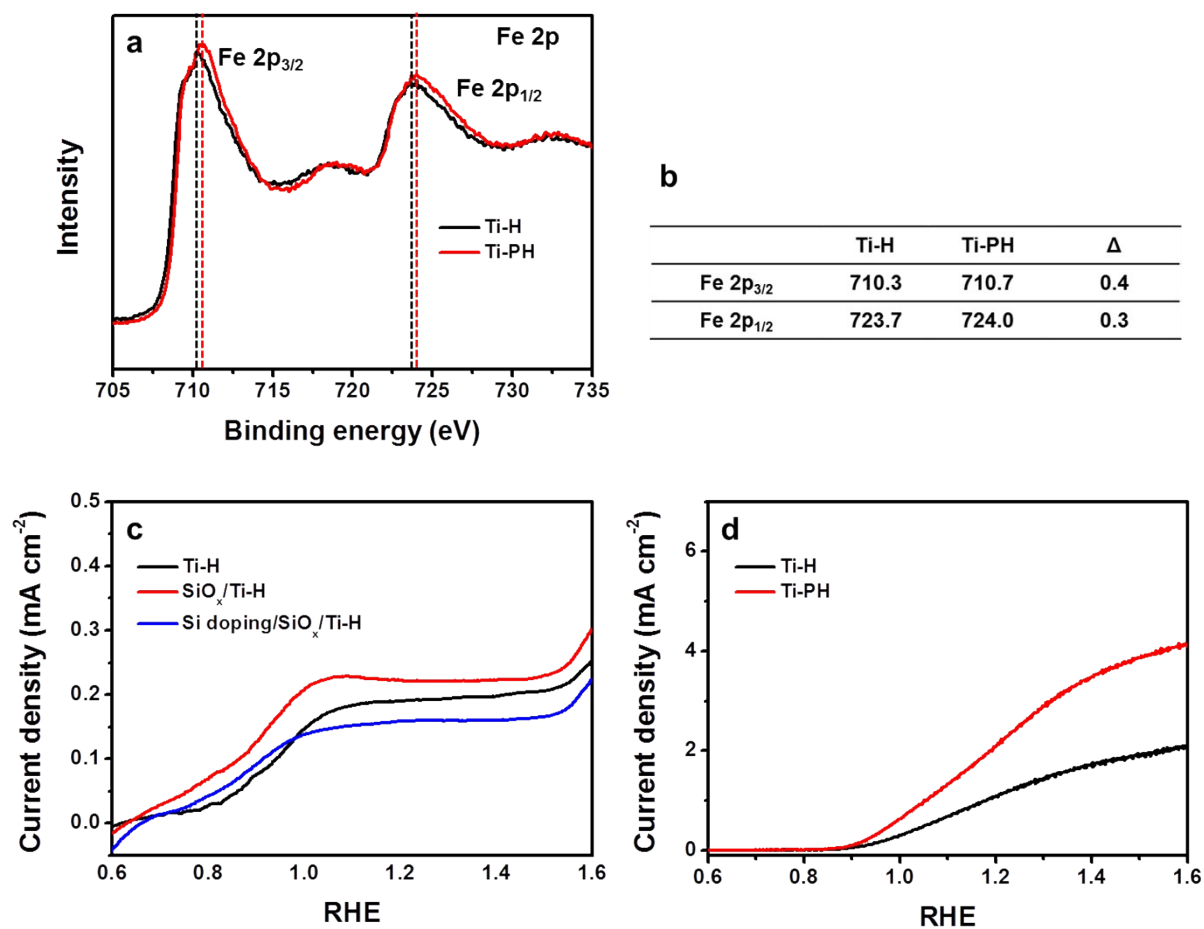


Figure S13. a) Fe 2P XPS spectra of Ti-H and Ti-PH. (b) Binding energy of Fe 2P_{3/2} and Fe 2P_{1/2}. J-V curves under simulated sunlight illumination (1 SUN) of c) the photoanode annealed at 550 °C (non-porous structure) and d) the photoanode with porous/nonporous structure (annealed at 850 °C).

The peak of Fe 2p_{3/2} and 2p_{1/2} was slightly shifted by 0.3-0.4 eV, which can be attributed to Si-doping in the Fe₂O₃ structure. However, Si-doping showed a negative effect in our limited study, by degrading the performance of Ti-PH, whereas the presence of the SiO_x passivation layer and porous structures positively affects the PEC performance.

[1] M. J. Kang, Y. S. Kang, J. Mater. Chem. A 3 (2015) 15723-15728.

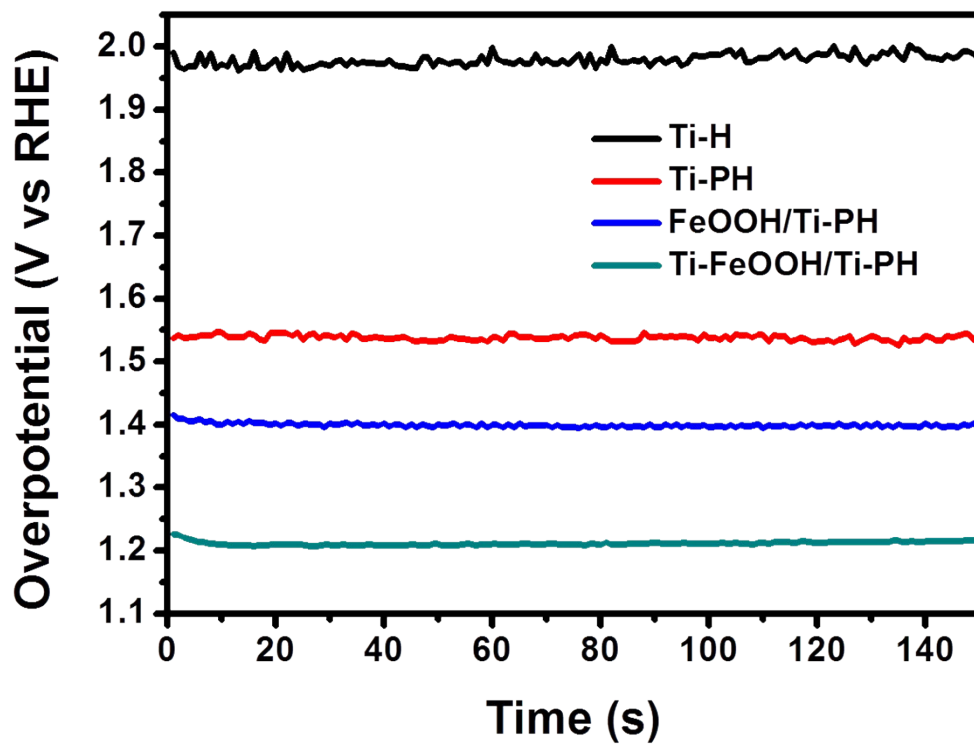


Figure S14. Potential (V vs. RHE) versus time plots at a current density of 4.0 mA cm^{-2} in a 1M NaOH electrolyte simulated sunlight illumination.

The potentials to generate current density of 4.0 mA cm^{-2} were 1.96 V (Ti-H), 1.54 V (Ti-PH), 1.40 V (FeOOH/Ti-PH), and 1.22 V (Ti-FeOOH/Ti-PH) vs RHE, which confirms the great performance of optimized Ti-FeOOH OER catalysts.

Table S1. The comparison of PEC efficiency of decent hematite-based water splitting systems.

Photoanode	Photocurrent density at 1.23 V vs RHE	Method	Reference (manuscript)
Sn-Fe₂O₃	1.86 mA cm ⁻²	Hydrothermal	[7] a
Co-Pi/Pt-Fe₂O₃	4.32 mA cm ⁻²	Hydrothermal/ Photo-assisted electrodeposition	[8] a
IrO₂/Fe₂O₃	Over 3 mA cm ⁻²	APCVD/electrodeposition	[8] b
Sn/Fe₂O₃	2.25 mA cm ⁻²	Hydrothermal	[9] b
Co-Pi/Fe₂O₃	2.8 mA cm ⁻²	APCVD/photo-assisted electrodeposition	[14] a
Al₂O₃/Si-Fe₂O₃	2.3 mA cm ⁻²	APCVD/ALD	[14] b
Co-Pi-Ti-(SiO_x/np-Fe₂O₃)	3.19 mA cm ⁻²	Hydrothermal and photo-assisted electrodeposition	[20]
Co-Pi/3D Ti-Fe₂O₃	3.05 mA cm ⁻²	Anodizing/vacuum vapor deposition/ Photo-assisted electrodeposition	[23] c
Ru-Fe₂O₃	5.7 mA cm ⁻²	Hydrothermal/doctor blading	[24]
Ti-FeOOH/Ti-PH	4.06 mA cm ⁻²	Hydrothermal	This study

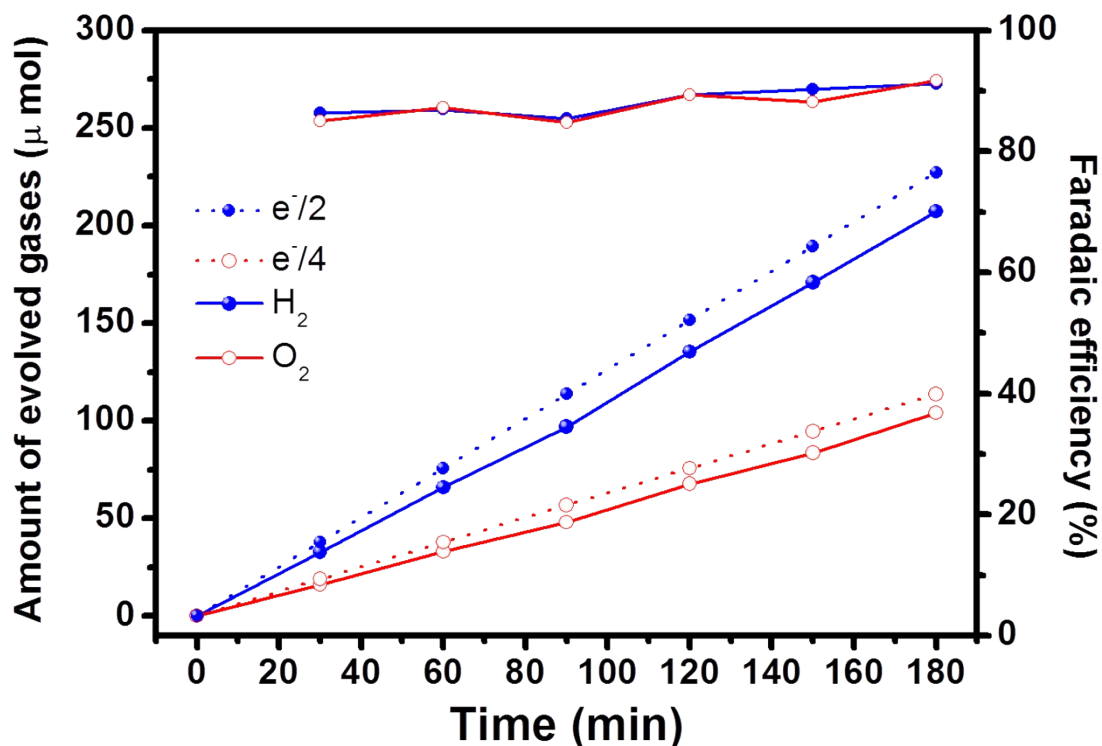


Figure S15. Faradaic efficiency of Ti-FeOOH/Ti-PH at 1.23 V vs RHE under AM 1.5 illumination in a 1 M NaOH electrolyte.

We calculated the faradaic efficiency on Ti-FeOOH/Ti-PH by measuring the H_2 and O_2 evolution using an H type cell at 1.23 V vs RHE under AM 1.5 illumination in 1 M NaOH electrolyte. As shown in Figure 5, the produced hydrogen gases on the Pt mesh and oxygen gases on Ti-FeOOH/Ti-PH are 207.2 μmol and 104.1 μmol after 180 min, respectively, indicating a 2:1 ratio of the water splitting mechanism. The ratio between the measured and predicted gas evolution rates gives a faradaic efficiency of 85-93% throughout the measurements. Therefore, most of the photo-generated charges were consumed for water splitting (hydrogen/oxygen gas generation) in our system.

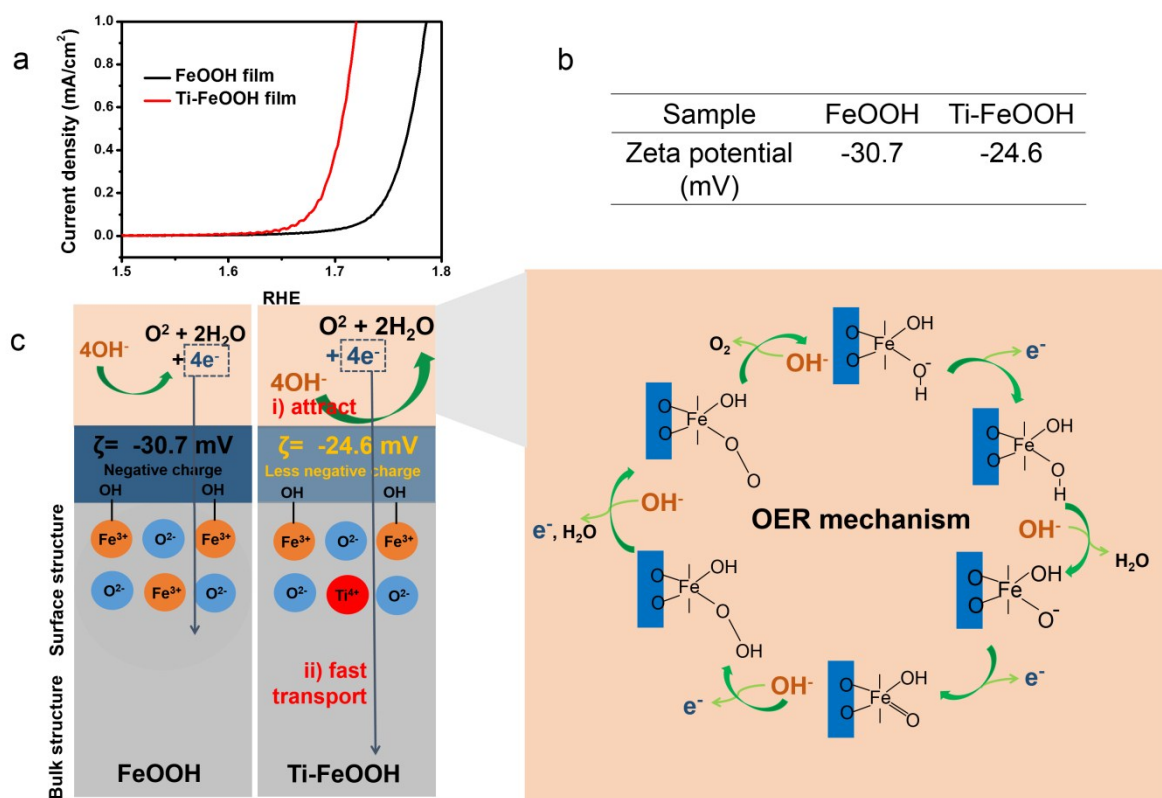


Figure S16. a) J-V curves in a 1 M NaOH (pH=13.6) electrolyte under the dark condition when the same density of FeOOH and Ti-FeOOH co-catalyst is tested. b) Zeta potential measurement. c) Schematic representation of the OER reactions catalyzed by FeOOH and Ti-FeOOH.

In order to suitably compare the OER property of FeOOH and Ti-FeOOH co-catalysts, we prepared FeOOH and Ti-FeOOH co-catalysts with the same density and obtained the J-V curves of each sample in a 1 M NaOH (pH=13.6) electrolyte under the dark condition. To obtain the same density of FeOOH and Ti-FeOOH co-catalyst, a high concentration of FeCl_3 (150 mM) was used to prepare the films rather than nanoparticles of FeOOH or Ti-FeOOH. As can be seen in the current density curves in Figure S13a, the OER property of Ti-FeOOH is much better than that of FeOOH in the dark condition. This can be explained by the different zeta potential value between Ti-FeOOH and FeOOH. FeOOH had an inherent negative zeta potential value (-30.7 mV) as shown in Figure S13b. However, Ti-FeOOH exhibited a less negative zeta potential value (-24.6 mV) due to the presence of the oxidation state of Ti^{4+} ions in the lattice. Ti-FeOOH with less negative potential is likely to better

facilitate the adsorption of OH⁻ than FeOOH in the electrolytes by shuttling more OH⁻ ions to the OER mechanism in Figure S13c, as in the previous report.^[1-3] Furthermore, Ti-FeOOH has better electrical conductivity than FeOOH, as demonstrated in Figure S13, which makes electrons generated during the OER reaction move fast through Ti-FeOOH. Therefore, Ti-FeOOH has better performance in the OER reaction than FeOOH.

[1] A. Minguzzi, O. Lugaresi, E. Achilli, C. Locatelli, A. Vertova, P. Ghigna, S. Rondinini, *Chem, Sci.* 5 (2014) 3591-3597.

[2] Y. Zhang, B. Ouyang, J. Xu, G. Jia, S. Chen, R. S. Rawat, H. J. Fan, *Angew. Chem. Int. Ed.* 128 (2016) 8812-8816.

[3] X. Lu, W-L. Yim, B. H. R. Suryanto, C. Zhao, *J. Am. Chem. Soc.* 137 (2015) 2901-2907.

Table S2. Fitted resistance values extracted from the impedance curves.

R/Ω cm²	R_{bulk}	R_{CT}
Ti-H	70.5	290.6
Ti-PH	55.5	188.0
FeOOH/Ti-PH	54.5	156.8
Ti-FeOOH/Ti-PH	48.1	132.4

As described in our previous report,^[1] Ti-PH showed lower recombination resistance inside the bulk material (R_{bulk}) than that of Ti-H, reflecting the suppression of recombination because of short pathways for the photogenerated holes. Further, Ti-FeOOH/Ti-PH showed a lower R_{bulk} value than that of FeOOH/Ti-PH. This implies easier charge transfer between co-catalysts and active materials, indicating that conductive Ti-FeOOH is more favorable to transfer photoexcited holes than FeOOH.

[1] H.-J. Ahn, K.-Y. Yoon, M.-J. Kwak, J.-H. Jang, *Angew. Chem. Int. Ed.* 5 (2016) 9922-9926.

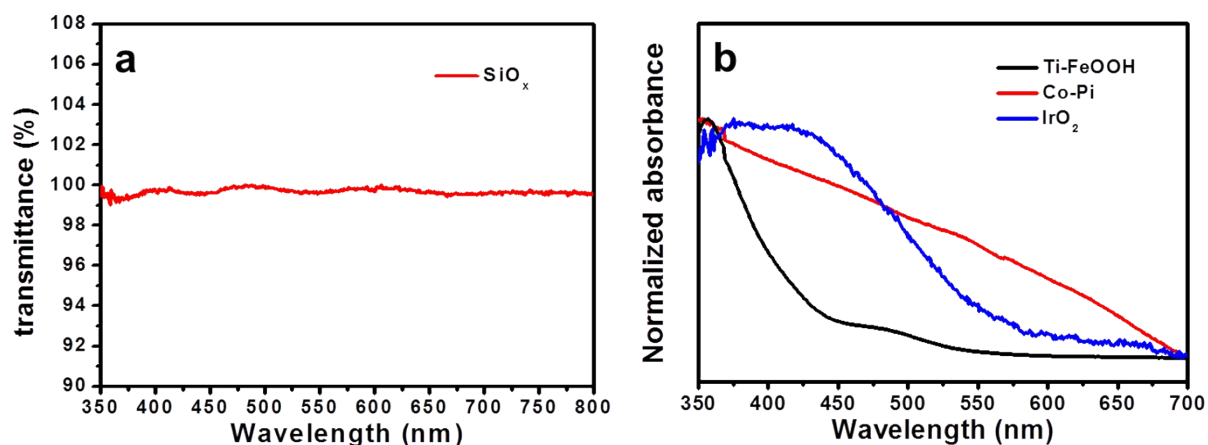


Figure S17. a) Transmission spectrum of the 5nm-thick SiO_x layer and b) absorption spectra of representative co-catalysts.

As can be seen in the optical property data of each component (SiO_x layer and co-catalysts) prepared with the same method as that employed for our PEC device, the SiO_x layer is highly transparent and representative co-catalysts (Co-Pi, IrO₂, and Ti-FeOOH) exhibit high absorption in the UV-VIS range that is not negligible. Thus, we can expect the presence of co-catalysts on the surface of hematite (rather than the thick SiO_x layer) more strongly affects the photo-catalytic properties of the active materials.

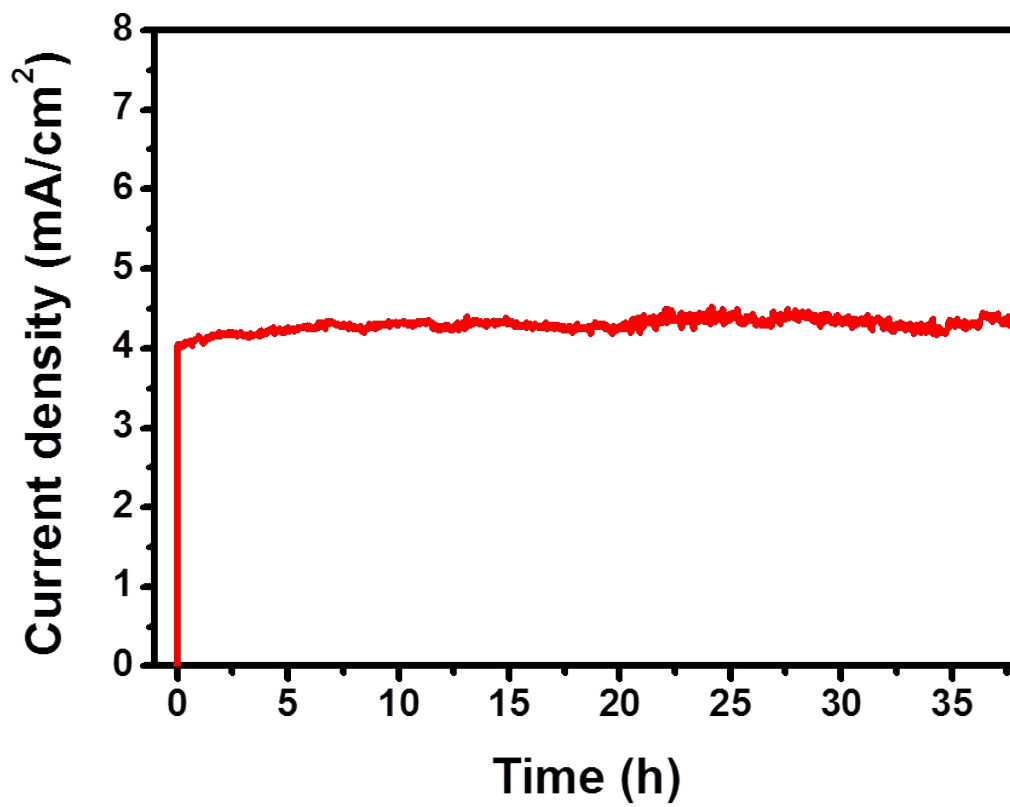


Figure S18. Long-term stability of Ti-FeOOH/Ti-PH.

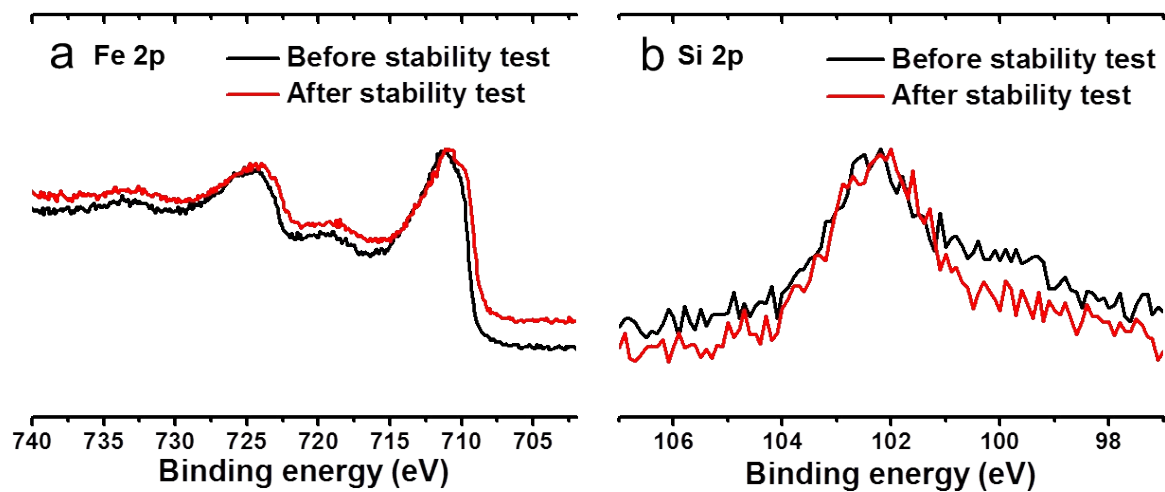


Figure S19. XPS spectra of Ti-FeOOH/Ti-PH before and after the 36 hrs' stability test. a) Fe 2p and b) Si 2p.